ARTICLE

BIOTECHNOLOGY and BIOENGINEERING

Permeable Reactive Biobarriers for In Situ Cr(VI) Reduction: Bench Scale Tests Using *Cellulomonas* sp. Strain ES6

Sridhar Viamajala,[1,2] Brent M. Peyton,[1,3] Robin Gerlach,[3] Vaideeswaran Sivaswamy,[1] William A. Apel,[4] James N. Petersen[1]

[1]Department of Chemical Engineering and Bioengineering, WSU/NSF IGERT Center for Multiphase Environmental Research, Washington State University, P.O. Box 642719, Pullman, Washington 99164-2719

[2]Department of Biological and Irrigation Engineering, 4105 Old Main Hill, Utah State University, Logan, Utah 84322-4105; telephone: 435-797-0217; fax: 435-797-1248; e-mail: sviamajala@cc.usu.edu

[3]Center for Biofilm Engineering, Chemical and Biological Engineering, Montana State University, Bozeman, Montana

[4]Biological Sciences Department, Idaho National Laboratory, Idaho Falls, Idaho

Received 18 March 2008; revision received 19 May 2008; accepted 20 May 2008

Published online 11 June 2008 in Wiley InterScience (www.interscience.wiley.com). DOI 10.1002/bit.22020

ABSTRACT: Chromate (Cr(VI)) reduction studies were performed in bench scale flow columns using the fermentative subsurface isolate *Cellulomonas* sp. strain ES6. In these tests, columns packed with either quartz sand or hydrous ferric oxide (HFO)-coated quartz sand, were inoculated with strain ES6 and fed nutrients to stimulate growth before nutrient-free Cr(VI) solutions were injected. Results show that in columns containing quartz sand, a continuous inflow of 2 mg/L Cr(VI) was reduced to below detection limits in the effluent for durations of up to 5.7 residence times after nutrient injection was discontinued proving the ability of strain ES6 to reduce chromate in the absence of an external electron donor. In the HFO-containing columns, Cr(VI) reduction was significantly prolonged and effluent Cr(VI) concentrations remained below detectable levels for periods of up to 66 residence times after nutrient injection was discontinued. Fe was detected in the effluent of the HFO-containing columns throughout the period of Cr(VI) removal indicating that the insoluble Fe(III) bearing solids were being continuously reduced to form soluble Fe(II) resulting in prolonged abiotic Cr(VI) reduction. Thus, growth of *Cellulomonas* within the soil columns resulted in formation of permeable reactive barriers that could reduce Cr(VI) and Fe(III) for extended periods even in the absence of external electron donors. Other bioremediation systems employing Fe(II)-mediated reactions require a continuous presence of external nutrients to regenerate Fe(II). After depletion of nutrients, contaminant removal within these systems occurs by reaction with surface-associated Fe(II) that can rapidly become inaccessible due to formation of crystalline Fe-minerals or other precipitates. The ability of fermentative organisms like *Cellulomonas* to reduce metals without continuous nutrient supply in the subsurface offers a viable and economical alternative technology for in situ remediation of Cr(VI)-contaminated groundwater through formation of permeable reactive biobarriers (PRBB).

Biotechnol. Bioeng. 2008;101: 1150–1162.

© 2008 Wiley Periodicals, Inc.

KEYWORDS: chromium; bioremediation; *Cellulomonas*; permeable reactive barrier; Cr(VI) reduction; chromate reduction; heavy metal; biofilm

Correspondence to: S. Viamajala

Contract grant sponsor: US Department of Energy, Office of Science, Natural and Accelerated Bioremediation Research (NABIR) Program (DOE-NE Idaho Operations Office)
Contract grant number: DE-AC07-05ID14517; DE-FG03-98ER62693
Contract grant sponsor: U.S. Department of Energy, Office of Science, Environmental Management Science Program (EMSP)
Contract grant number: DE-FG02-03ER63577; DE-FG02-03ER63582; DE-FG02-06ER64206
Contract grant sponsor: Inland Northwest Research Alliance
Contract grant number: WSU 005; MSU 002

Introduction

In natural environments, chromium is found in trivalent [Cr(III)] and hexavalent [Cr(VI)] forms. Cr(VI) is highly soluble and mobile (Dragun, 1988), and enters the environment due to anthropogenic uses (Langard, 1980; Patterson, 1985; Riley et al., 1992). At low concentrations, typical of those found in the environment, the chronic health effects of hexavalent chromium compounds are insidious, as Cr(VI) has both mutagenic and carcinogenic effects (DeLeo and

© 2008 Wiley Periodicals, Inc.

Ehrlich, 1994; World Health Organization, 1990). Cr(III), on the other hand, often exists as chromium hydroxides which are only slightly soluble, have a high soil partition coefficient, and are therefore much less mobile (Barnhart, 1997; Richard and Bourg, 1991). In addition, Cr(III) is much less toxic and is, in fact, an essential nutrient and a popular dietary supplement (Stearns et al., 1995).

In situ microbial reduction of Cr(VI) to Cr(III) is one potential treatment technology for remediation of Cr(VI) contamination. In previous studies, Cr(VI)-reducing microorganisms were found in diverse locations indicating that enzymatic Cr(VI) reducing capability is likely widespread among bacteria (Schmieman et al., 1998; Turick et al., 1996). However, most studies have focused on Gram negative organisms such as those belonging to the genera *Pseudomonas*, *Desulfovibrio*, *Shewanella*, and *Escherichia* (Ackerley et al., 2004; Chardin et al., 2003; Viamajala et al., 2002 and references therein). In contrast, our enrichments from contaminated and uncontaminated aquifers at the U.S. Department of Energy (DOE) Hanford site showed several Gram positive *Cellulomonas* strains (Sani et al., 2002; Viamajala et al., 2007), indicating that fermenting communities containing organisms such as *Cellulomonas*, may contribute significantly to in situ Cr(VI) reduction.

Cr(VI) reduction through rapid abiotic reaction with ferrous iron [Fe(II)], is an alternate route for remediation of Cr(VI) (Wielinga et al., 2001). Besides Cr(VI), the rapid and non-specific electron transfer from Fe(II) can be applied for remediation of other redox active contaminants such as, radionuclides (e.g., U(VI)), chlorinated aliphatics (e.g., carbon tetrachloride and trichloroethylene), and nitroaromatics (e.g., 2,4,6-trinitrotoluene) (Amonette et al., 2000; Borch et al., 2005; Erbs et al., 1999; Fredrickson et al., 2000a; Lee and Batchelor, 2002). In the subsurface, Fe(II) can be generated by the reduction of ferric [Fe(III)] minerals, either by addition of reductants such as dithionite (Chilikapati et al., 2000; Istok et al., 1999) or by action of microorganisms (Heijman et al., 1995). Injection of chemicals to produce Fe(II) depends on regulatory approval and likely incurs large chemical costs and expenses for disposal of secondary waste (Chilikapati et al., 2000). In contrast, generation of Fe(II) by stimulating indigenous Fe(III)-reducing organisms is likely to encounter fewer regulatory hurdles, and can potentially be less expensive, especially if economical nutrient sources such as molasses or cheese whey are used.

Microbial Fe(III) reduction is most commonly studied with dissimilatory iron reducing bacteria (DIRB) such as those belonging to the genera *Geobacter* or *Shewanella*. However, Fe(III) reduction is also common among fermenting, sulfate-reducing, halorespiring, and methanogenic bacteria, all of which are able to reduce both dissolved and solid phase Fe(III), either through direct enzymatic mechanisms or indirectly though electron shuttles such as humic acids or their analogs (Benz et al., 1998; Cervantes et al., 2002; Lovley et al., 1991). While most organisms appear to require a continuous supply of electrons from an external carbon source to reduce Fe(III), our studies show that *Cellulomonas* isolates can reduce Cr(VI) and soluble Fe(III) for prolonged periods (>3 months) in the absence of external electron donors (Sani et al., 2002; Viamajala et al., 2007). In addition, these organisms can reduce Fe(III) from crystalline as well as amorphous Fe-minerals such as hydrous ferric oxide (HFO), goethite, maghemite, hematite, and magnetite (unpublished data). These results suggest that if *Cellulomonas* spp. or similar organisms are stimulated in the subsurface, they could maintain in situ Fe(III) reduction without continuous injection of nutrients, thus forming reactive barriers for contaminant remediation. In the present study, we performed bench scale flow-through soil column experiments to test the feasibility of generating reducing biobarriers for Cr(VI) remediation using *Cellulomonas* sp. strain ES6 (henceforth referred to as ES6). Our results show that once ES6 was stimulated in the columns, Fe(III) reduction and concomitant Cr(VI) reduction continued for up to 66 pore volumes without addition of any external nutrients. In addition, after depletion of Cr(VI) reducing activity, metal reduction in the columns could be restored to previous levels by re-addition of nutrients.

Materials and Methods

Microorganism and Culture Conditions

ES6 was isolated from a Cr(VI) contaminated aquifer at the US DOE Hanford site as previously reported by Viamajala et al. (2007). The culture was revived from frozen stocks (−80°C in 20% glycerol) by growing cells aerobically to late log phase on 30 g/L Tryptic Soy Broth medium (TSB, Difco, BD Diagnostic Systems, Sparks, MD) and transferring them twice into fresh medium to remove glycerol. Late log phase TSB-grown cultures of ES6 were used as inoculum for the column experiments. All batch cultures were grown at 25°C on a gyratory shaker at 125 rpm.

Experimental System

Traditional-Hydro-Purge® moisture trap columns from Alltech Associates, Inc. (Deerfield, IL) were modified and used as columns in our experiments. The transparent acrylic polymer columns were 17 cm long with an internal diameter of 2.5 cm. Before use, the original desiccant in the column was removed and the columns were thoroughly washed. A stainless steel (SS) screen and a flow distributor were placed at the column entrance to support the matrix and minimize short-circuiting. Flow was delivered through a multichannel syringe pump (Model KDS220, KD Scientific, Inc., Holliston, MA) using 140 mL syringes. A maximum of 2 columns were operated with each pump to prevent pump failure due to backpressure. The syringes were connected to sterile 0.2 μm syringe filters (Millipore, Bedford, MA) and

then 1/8 inch SS needles and tubing leading to the columns. Effluent was also removed through 1/8 inch SS tubing.

Column Start-Up and Operation

The purpose of this study was to investigate Cr(VI) reduction by ES6 in porous media flow-through reactors by direct enzymatic and Fe(II)-mediated mechanisms in the absence of external electron donors. Consequently, duplicate tests were performed with columns containing washed quartz sand and HFO-coated sand. Sandblasted quartz sand (Lane Mountain Company, Valley, WA) with an average particle size of 420 μm was washed with 1 N HNO_3 to remove residual metal, rinsed with de-ionized (DI) water and dried before use. Part of the sand was coated with HFO using the method described by Nyman et al. (2002). The uncoated and HFO-coated sands were pasteurized by incubation in an oven at 80°C for at least 4 h before use in our experiments. Columns, accessory tubing and syringes were sterilized by autoclaving (121°C, 15 min) before use.

To inoculate the columns, approximately 45 mL of TSB-grown late log phase ES6 cultures were poured into the empty sterile columns and the rest of the volume was filled with pasteurized sand. The columns were gently vortexed at several stages during pouring to achieve uniform packing and all maneuvers were performed aseptically in a laminar flow hood. After inoculation, the columns were capped and connected to sterile tubing and syringes of the flow-through system. The columns were allowed to stand for 24 h to facilitate microbial attachment to the solid phase before nutrient flow was started.

Columns were operated in two phases: (1) growth phase and (2) Cr(VI) reduction phase. In the growth phase, simulated groundwater medium (SGM) containing nutrients was pumped through the columns to stimulate ES6 growth. The flow rate during the growth phase was maintained at relatively high levels of 13.2 mL/h to facilitate nutrient distribution throughout the column and prevent excessive biomass accumulation near the column entrance. SGM in the growth phase contained (per L of medium): sucrose ($C_{12}H_{22}O_{11}$) (500 mg), $CaCl_2 \cdot 2H_2O$ (8 mg), $MgCl_2 \cdot 2H_2O$ (75 mg), $NaHCO_3$ (2,520 mg), Na_2SO_4 (6 mg), KCl (26.5 mg), Na_2SiO_3 (100 mg), yeast extract (50 mg), anthraquinone-2,6-disulfonate (AQDS) (20 mg), and 0.1 mL of a trace element stock solution. The trace element stock was prepared by dissolving the following in 1 L of 75 mM phosphoric acid: LiCl (21 mg), $CuSO_4 \cdot 5H_2O$ (80 mg), $ZnSO_4 \cdot 7H_2O$ (106 mg), H_3BO_4 (600 mg), $Al_2(SO_4)_3 \cdot 18H_2O$ (123 mg), $NiCl_2 \cdot 6H_2O$ (110 mg), $CoSO_4 \cdot 7H_2O$ (109 mg), Na_2SeO_4 (50 mg), $MnCl_2 \cdot 4H_2O$ (629 mg), KBr (30 mg), KI (30 mg), Na_2MoO_4 (10 mg), $FeSO_4 \cdot 7H_2O$ (300 mg). In SGM, sucrose and yeast extract served as carbon and nutrient sources, bicarbonate served as buffer (30 mM), and AQDS was added as a humic acid analog. After 2 weeks of growth, Cr(VI) was fed to the reactors. During this Cr(VI) reduction phase, sucrose and yeast extract were not added, and instead, the SGM was supplemented with 2 mg/L Cr(VI) (as K_2CrO_4). Also, a lower flow rate of 1.32 mL/h was used during this phase to more accurately represent actual groundwater velocities.

SGM was prepared in 500 mL serum bottles (Wheaton Science Products, Millville, NJ), sealed with rubber septa and aluminum foil caps, and autoclaved. After cooling, the bottles were purged with N_2/CO_2 (80:20) for 30 min to remove oxygen, pressurized to 20 psig and equilibrated in the N_2/CO_2 atmosphere for 8–12 h. Then, the medium was filled into syringes, while being purged with N_2/CO_2, and this procedure resulted in an anoxic feed at pH 7.2.

Sampling

During the experiment, effluent samples were collected in sealed sterile vials attached to the effluent tubing. Part of the sample was filtered using 0.2 μm syringe filters (Millipore) and analyzed for sucrose, Cr(VI), total-Cr (Cr_{tot}), and total-Fe (Fe_{tot}). Unfiltered effluent samples were used for counting colony-forming units (CFU). After completion of the experiments, sealed columns were transferred into an anaerobic glove box (Model 1025, Forma Scientific, Inc., Marietta, OH; gas mix—90% N_2, 5% H_2, and 5% CO_2) where the column contents were gently extruded and segmented. Shorter segment lengths (0.5–1 cm) were used at the influent half of the columns since it was expected that a larger portion of the biological activity would be near the inlet. The other half was divided into 2 cm long segments. The solids within each segment were thoroughly mixed with a spatula and duplicate samples from each segment were analyzed for protein content, Cr_{tot}, Fe(II), and Fe_{tot}.

Tracer Tests

Duplicate bromide and Cr(VI) tracer tests were performed on un-inoculated quartz and HFO columns (packed using sterile DI water) to determine hydrodynamic properties within the columns and to assess Cr(VI) sorption to the packing material under our experimental conditions. For the bromide tracer studies, a 100 mg/L KBr solution in DI water was continuously pumped through the columns, and effluent bromide concentrations were monitored. During the bromide tracer tests, the flow rate was maintained at 13.2 mL/h to represent flow during the growth phase. For the Cr(VI) tracer studies, sterile SGM was first pumped through the columns for 7 days before introduction of the Cr(VI) tracer, to simulate actual experimental conditions of growth followed by Cr(VI) reduction. The flow rate used in the Cr(VI) tracer tests was 1.32 mL/h and the influent concentration was 2 mg/L, analogous to conditions used in the Cr(VI) reduction phase with inoculated columns.

Tracer data were analyzed using the following convection–dispersion model previously used by Rege et al. (1998)

$$\frac{\partial C_i}{\partial t} = D_L \frac{\partial^2 C_i}{\partial x^2} - u \frac{\partial C_i}{\partial x} \quad (1)$$

where C_i is the concentration of species i, D_L is the dispersion coefficient and u is the liquid velocity through the column. Using the initial and boundary conditions: $C_i(x,0) = 0$, $C_i(0,t) = C_0$, and $dC_i(L,t)/dt = 0$, an analytical solution of Equation (1) can be given as (Rege et al., 1998):

$$\frac{C_i}{C_0} = \frac{1}{2}\left[1 - \mathrm{erf}\left\{\frac{1}{2}\sqrt{Pe}\left(\frac{1-(t/\tau)}{\sqrt{t/\tau}}\right)\right\}\right] \quad (2)$$

where, C_0 is the influent concentration, L is the length of the column, Pe is the Peclet number (uL/D_L), τ represents the residence time and is given by the ratio L/u, and erf is the error function value. u can be related to the volumetric flow rate into the column (V), cross sectional area of the column (A), and the column porosity (ε) using the relation $u = V/A\varepsilon$. Experimental tracer data were fitted to Equation (2) using the Solver function in Microsoft Excel©, by varying the Peclet number and column porosity to minimize the sum of the squared differences between the observed and predicted tracer concentrations.

Analytical Methods

Iron

Fe_{tot} in the effluent liquid was measured by the Hach FerroVer® method (Hach Company, Loveland, CO) as described previously by Sani et al. (2002). Periodically, effluent samples were allowed to flow for 10 min directly into 220 μL of 1 N HCl contained in microcentrifuge tubes (to prevent oxidation of Fe(II)) and Fe(II) concentrations were measured using the ferrozine method (described below). During these measurements, Fe(II) and Fe_{tot} concentrations were observed to be very similar.

At the end of the experiments, Fe_{tot} and Fe(II) in the solid phase were also determined using the ferrozine method. For Fe(II) analysis, 0.1–0.2 g of wet solids from each column segment were extracted with 1 mL of 0.5 or 2.5 M HCl in pre-weighed microcentrifuge tubes, in accordance with previously described methods (Lovley and Phillips, 1987; Nyman et al., 2002). Fe_{tot} measurements were made after extracting the solids in 0.5 M and 2.5 M HCl solutions containing 0.25 M hydroxylamine (NH_2OH) as reductant, while keeping the solids to liquid ratio the same as that for Fe(II) extractions. The 0.5 M HCl extractions were performed for 2 h, and other extractions were done for at least 12 h under static conditions with intermittent mixing. Fe measurements were performed by adding 20 μL of acid extract to 180 μL of 1 g/L ferrozine solution in 96-well microtiter plates (Corning, Inc., Corning, NY) and measuring the absorbance at 562 nm using a microplate reader (HTS 7000 Bio Assay Reader, Perkin Elmer, Norwalk, CT). When the absorbance values were above measurable limits, the extracts were suitably diluted into corresponding acid solutions before measurement. The ferrozine solution was made in 50 and 750 mM HEPES buffer (pH 7), for low and high acid concentration extract analyses, respectively. After extraction and Fe analysis, dry weights of the sand were measured by drying at 105°C for 12 h. Measured solid phase Fe values are reported as mg Fe per g of dry sand.

Chromium

Cr(VI) in the effluent liquid was measured by the diphenylcarbazide method using the Hach ChromaVer 3 reagent (Hach Company) as described previously by Viamajala et al. (2002). For solid phase analysis, Cr was first extracted from approximately 1 g wet samples with 5 mL of 1 N HNO_3 for 12 h, and a part of the extract was analyzed for Cr(VI) as described above. The rest of the extract was further diluted with the same strength acid (200 μL sample or standard + 3,800 μL acid) and Cr_{tot} was measured by Inductively Coupled Plasma-Mass Spectrometry (ICP-MS) (model 4500 Agilent Technologies, Palo Alto, CA). Effluent samples and Cr standards were similarly diluted in 1 N HNO_3 and analyzed for Cr_{tot}. Cr(III) was calculated as the difference between Cr_{tot} and Cr(VI).

Protein

Cell protein concentrations on the sand were determined by a modification of the Bradford method (Bradford, 1976). Approximately 1 g of wet solid sample was mixed with 2 mL of 0.5 M NaOH, thoroughly vortexed, and incubated at 90°C for 20 min to disrupt cells and release intracellular protein. After cooling, the sample was acidified using 0.2 mL of 6 M HCl. Acidified sample (100 μL) was mixed with 100 μL of Coomassie® Plus Protein Assay Reagent (Pierce Chemical Company, Rockford, IL) in 96-well microtiter plates and the absorbance was measured at 595 nm. Calibrations were performed using a 2 mg/mL bovine serum albumin (BSA) standard (Pierce Chemical Company) diluted with DI water to a concentration range of 0–50 mg/L. One milliliter of diluted standards was mixed with 1 mL of 1 N NaOH, heated, acidified and assayed along with samples.

CFU Counts

CFU counts were performed using Tryptic Soy Agar (Difco) plates after serial dilution of effluent samples in 30 mM phosphate buffered saline solution. These measurements also served to indicate if there were other organisms besides ES6 in the columns and in our experiments; we did not observe evidence of contamination.

Bromide

Bromide concentrations were measured using a conductivity meter (Orion 105Aplus, Thermo Electron Corporation, Beverly, MA). Since tracer tests were performed with pure bromide solutions in DI water, conductivity values could be directly correlated to bromide concentrations.

Statistical Analysis

Effluent CFU counts as well as solid phase Fe(II), total Fe, total Cr and protein measurements were performed in triplicate for each sample. Standard deviations and 95% confidence intervals of means were calculated using MS Excel©.

Results

Tracer Tests

Data from all replicate bromide and Cr(VI) tracer tests are shown in Figure 1. Peclet number and porosity were estimated from each tracer test using Equation (2), and mean values of parameters for bromide and Cr(VI) tracers are shown in Table I along with other calculated hydrodynamic properties. Mean parameter values were then used in Equation (2), to calculate effluent concentrations as a function of time for the two tracers. These results, represented by solid lines in Figure 1A and B, show that model predictions for residence time distribution correspond closely to experimental observations. Further, the porosity estimates matched closely between bromide and Cr(VI) tracers (Table I) and the calculated residence times were proportional to the flow velocity, indicating that Cr(VI) was not significantly retarded by the quartz- and HFO-coated sand matrices. The high Peclet number values (>50) also suggest low dispersion and nearly ideal plug flow conditions (Burton et al., 2003).

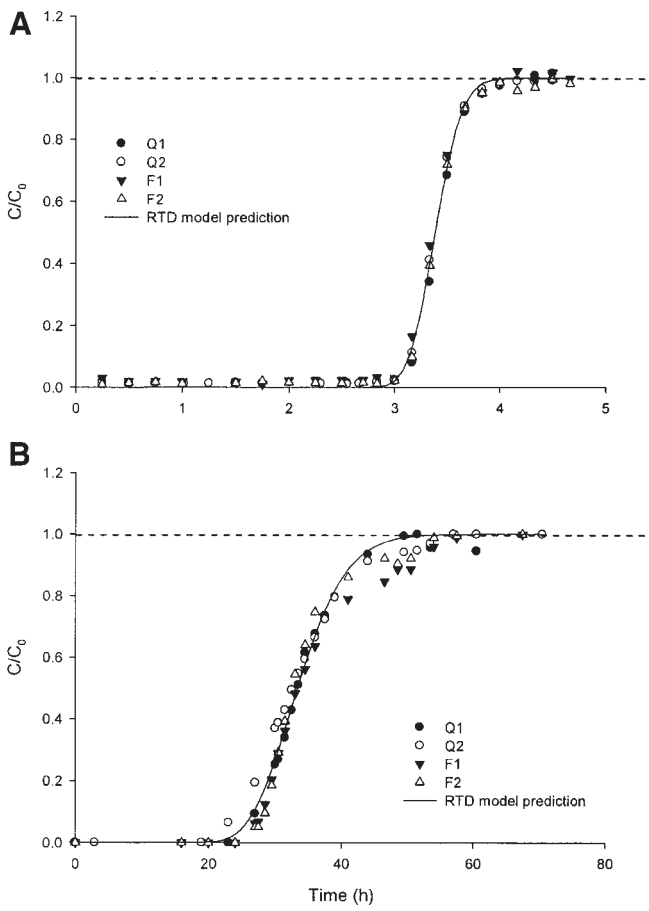

Figure 1. (**A**) Bromide and (**B**) Cr(VI) tracer data for quartz sand (Q1 and Q2) and HFO-coated sand (F1 and F2) columns.

Table I. Summary of hydrodynamic flow properties estimated from tracer tests.

Parameter	Bromide tracer tests	Cr(VI) tracer tests
Volumetric flow rate (cm^3/h)	13.2	1.32
Porosity	0.536 ± 0.003	0.528 ± 0.012
Flow velocity (cm/h)	5.02 ± 0.03	0.51 ± 0.01
Peclet number	580.7 ± 62.6	67.7 ± 33.0
Residence time (h)	3.38 ± 0.02	33.36 ± 0.76

Errors indicate 95% confidence intervals.

Effluent Data—Quartz Columns

Effluent CFU, Cr(VI) and total-Cr concentrations for replicate quartz sand-containing columns (labeled Q1 and Q2) are shown in Figure 2. After inoculation on day 0, the columns were fed with nutrients during days 0–13 in the absence of Cr(VI) (growth phase I). Sucrose was consumed during this period (Fig. 3A) and relatively high effluent cell concentrations measured (approximately 1e7 CFU/mL, Fig. 2), indicating growth of ES6. After day 13, nutrient addition was stopped and Cr(VI), at 2 mg/L, was injected into the columns. Effluent Cr(VI) concentrations stayed below detection limits between 14 and 22 days for both columns Q1 and Q2 (Fig. 2). Based on an average residence time of 33.4 h calculated from tracer data (Table I), this corresponds to complete Cr(VI) reduction for a period of 5.7 residence times (τ) (Table II). After breakthrough on day 22, Cr(VI) concentrations stayed below influent concentrations until day 35 for both Q1 and Q2, indicating that partial Cr(VI) reduction continued for another 9.3τ (Table II). Also, during this Cr(VI) reduction phase, effluent CFU concentrations decreased to <1e6 CFU/mL, indicating that the active cell population within the column had significantly decreased. Another observation from Figure 2 is that effluent total-Cr levels stayed higher than Cr(VI), indicating the formation of soluble Cr(III) (Alam et al., 2006).

To test if Cr(VI) reduction activity could be restored by re-growing the organisms, nutrient addition to Q1 and Q2

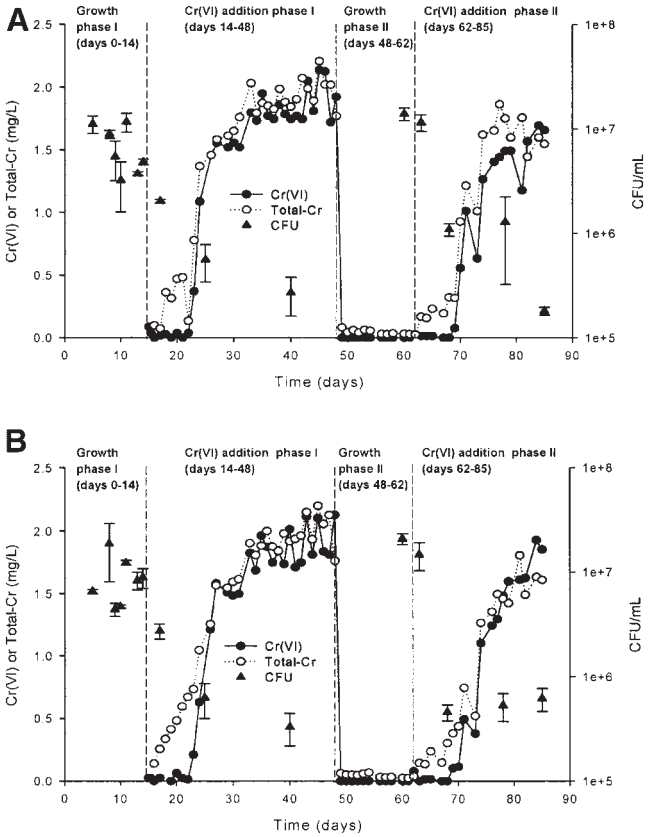

Figure 2. Effluent Cr(VI), total-Cr and CFU data for quartz sand columns (**A**) Q1, and (**B**) Q2. Error bars on CFU counts indicate 95% confidence intervals of mean values from triplicate measurements.

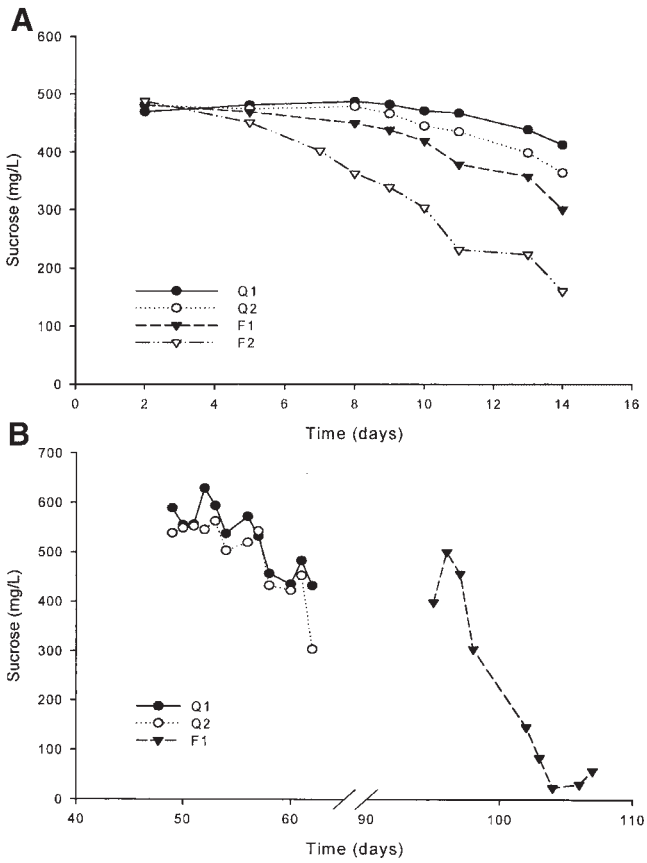

Figure 3. Effluent sucrose data for (**A**) nutrient addition phase 1, and (**B**) nutrient addition phase 2. Q1 and Q2 represent data from the quartz sand columns, while F1 and F2 represent data from the HFO-coated sand columns.

was re-started on day 48 and continued for 14 days until day 61. Resumption of nutrient feed led to sucrose consumption (Fig. 3B) and an increase in effluent cell concentrations (>1e7 CFU/mL, Fig. 2), indicating re-growth of ES6. After day 61, nutrient addition was stopped and Cr(VI) injection was re-started. No Cr(VI) was detected in the effluents until day 69, corresponding to complete Cr(VI) reduction for 5.0τ (Table II). After Cr(VI) breakthrough, the cultures continued partial Cr(VI) reduction and effluent Cr(VI) concentrations did not appear to reach influent levels until day 84 for Q2 (10.8τ). Cr(VI) concentrations in the effluent of Q1 never reached influent levels during the 85-day duration of the experiment. Also, similar to results obtained during the previous Cr(VI) addition phase, effluent cell concentrations decreased to <1e6 CFU/mL (Fig. 2) and total-Cr in the effluent was measured to be higher than Cr(VI), again indicating the formation of soluble Cr(III).

Effluent Data—HFO-Coated Sand Columns

Replicate columns containing HFO-coated sand (named F1 and F2) were tested for the potential of Fe minerals to enhance the performance of the biobarrier due to Fe(II)-mediated Cr(VI) reduction. Like previous tests with the quartz columns, nutrients were fed to F1 and F2 for a period of 14 days to stimulate growth of ES6. During this growth period, as observed for the quartz columns, effluent cell concentrations were measured to be >1e7 CFU/mL (Fig. 4) and sucrose consumption was observed. More sucrose was consumed in F2 compared to F1 (Fig. 3), likely resulting in higher cell growth in F2.

After 14 days, the sucrose feed was stopped and Cr(VI) was fed to F1 and F2. Corresponding to the higher sucrose consumption in F2, Fe(III) reduction was greater in this column such that the highest effluent Fe concentration measured was 14.6 mg/L on day 30 (Fig. 5). Although much lower Fe was measured in F1 effluent samples, it is interesting to note that the maximum Fe concentration from this column (2.5 mg/L) was also measured on day 30. It is likely that this lag in Fe release from the columns is due to retardation of Fe(II) within the column due to sorption on the mineral surface. After day 30, Fe concentrations in the effluents from both columns decreased steadily and were below the detection limit (0.05 mg/L) on days 52 and 98 for F1 and F2, respectively.

Table II. Summary of durations of complete and partial Cr(VI) reduction.

	Duration of complete Cr(VI) reduction ($\times\tau$)		Duration of partial Cr(VI) reduction ($\times\tau$)	
Column	Cr(VI) reduction phase 1	Cr(VI) reduction phase 2	Cr(VI) reduction phase 1	Cr(VI) reduction phase 2
Q1	5.7	5.0	9.3	10.8
Q2	5.7	5.0	9.3	>10.8
F1	26.6	66.1	22.3	15.1
F2	60.4	n/a	21.5	n/a

τ, average hydraulic residence time.

Appearance of Cr(VI) in the effluent corresponded closely with disappearance of effluent Fe such that Cr(VI) breakthrough occurred on days 52 and 98 for F1 and F2, respectively (Fig. 4). Based on the column residence time (33.4 h), breakthrough occurred after 26.6τ and 60.4τ for F1 and F2, respectively (Table II). There appears to be an earlier breakthrough of total Cr, beginning at around day 33 for column F1 and day 35 for column F2, possibly indicating the presence of soluble Cr(III) compounds (Alam et al., 2006). Following breakthrough of Cr(VI), partial Cr(VI) reduction continued and Cr(VI) concentrations in the effluent stayed in the range of 1.4–1.7 mg/L between days 52 and 84 for column F1 (equivalent to 22.3τ of partial Cr(VI) reduction) and between days 98 and 128 for column F2 (21.5τ of partial Cr(VI) reduction, Fig. 4 and Table II). Effluent cell concentrations were also observed to be approximately 1e6 CFU/mL (Fig. 4) and thus similar to those observed in the quartz columns during Cr(VI) reduction.

In order to regenerate F1, similar to the quartz columns, nutrients were re-fed for 14 days after day 95. As observed in the quartz sand columns, the re-addition of nutrients to F1 led to sucrose consumption (Fig. 3B) and an increase in effluent cell concentration (>1e7 CFU/mL, Fig. 4A). In fact, higher levels of sucrose utilization were observed during this

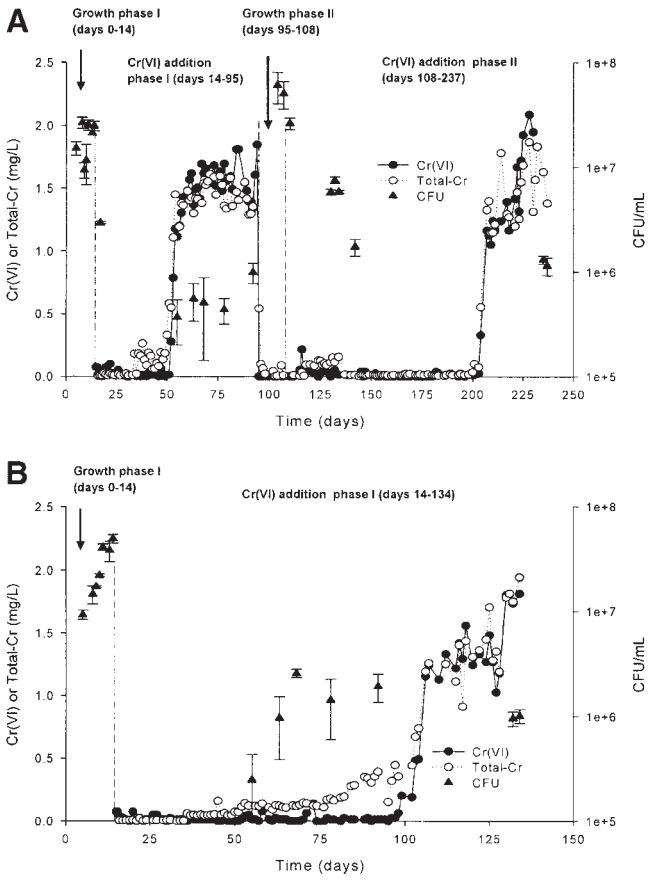

Figure 4. Effluent Cr(VI) and total-Cr data for HFO-coated sand columns (**A**) F1 and (**B**) F2. Error bars on CFU counts indicate 95% confidence intervals of mean values from triplicate measurements.

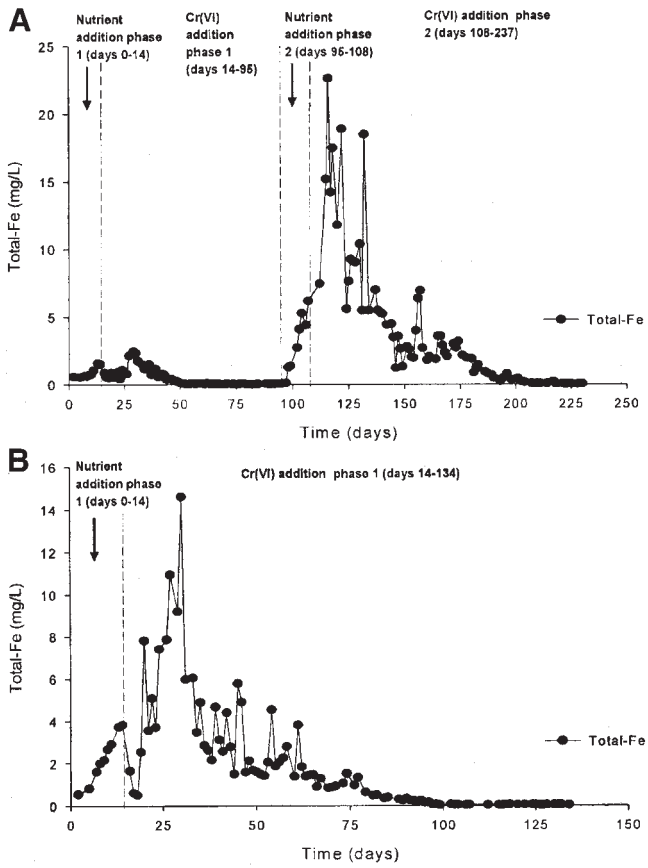

Figure 5. Effluent total-Fe data for HFO-coated sand columns (**A**) F1 and (**B**) F2.

nutrient addition cycle in comparison to the previous addition (Fig. 3B) indicating that high cell growth occurred within the column. Correspondingly, Fe concentrations in the effluent were also higher such that a maximum concentration of 22.6 mg/L was measured on day 116; 8 days after nutrient flow was discontinued. Thereafter, effluent Fe concentrations decreased and were below detectable levels on day 204 (Fig. 5). Analogous to the previous Cr(VI) addition phase with F1 and F2, Cr(VI) breakthrough coincided with the disappearance of Fe in the effluent and occurred on day 204. Thereafter, partial Cr(VI) reduction continued until day 225. Thus, during this second Cr(VI) reduction phase with F1, the durations of complete and partial Cr(VI) reduction were 66.1τ and 15.1τ, respectively. Effluent cell concentrations decreased to approximately 1e6 CFU/mL during this test as well, but total-Cr values remained close to Cr(VI) concentrations for most of the run (Fig. 4B), indicating little, if any, soluble Cr(III).

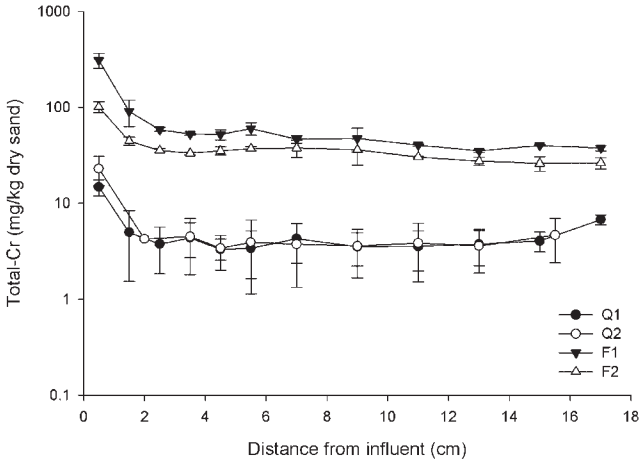

Figure 7. Solid phase total-Cr profiles for all columns. Error bars indicate 95% confidence intervals of mean values from triplicate measurements.

Solid Phase Data

Figure 6 shows cell protein concentrations within the column as a function of column length after completion of the experiments. Protein concentrations for Q1 and Q2 were more similar as would be expected from similar sucrose consumption and Cr(VI) reduction observed with these columns. Apart from the slightly higher protein levels observed near the influent, the attached cell concentrations appeared to be relatively uniform throughout the rest of the column length. The F-columns had a higher protein concentration than the Q-columns and concentrations were much higher in F1 than F2, likely since F1 was fed nutrients twice and more sucrose was consumed. It can also be observed from Figure 6 that the protein concentrations in the F-columns were higher near the influent but stayed relatively uniform for the remaining length of the columns.

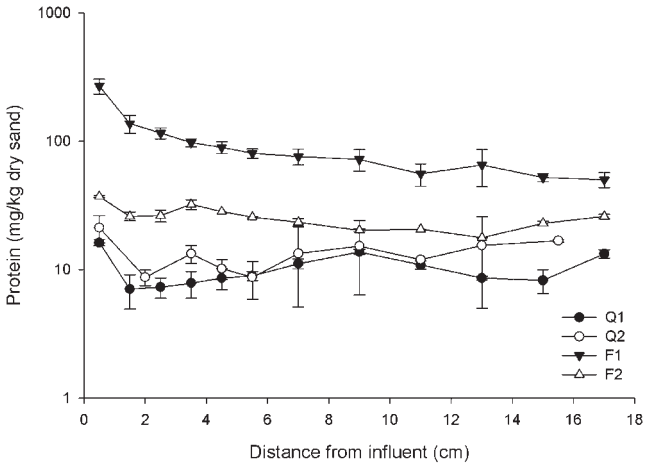

Figure 6. Solid phase protein profiles for all columns. Error bars indicate 95% confidence intervals of mean values from triplicate measurements.

Figure 7 shows solid phase Cr within all columns at the end of the experiment. More Cr was present at the influent, correlating to higher protein concentrations in this region (Fig. 6). The F-columns had much higher Cr levels than the Q-columns, in accordance with much higher Cr(VI) reduction observed in these columns.

Profiles of extractable Fe from columns F1 and F2 are shown in Figure 8. The concentrations of the 0.5 N HCl extracts, which yields "easily dissolved" or "mild acid extractable" Fe(II) (Lovley and Phillips, 1987; Nyman et al., 2002), were observed to be the lowest. This is expected since most of this Fe(II) would have been consumed during Fe(II)-mediated Cr(VI) reduction in the column. However, since some 0.5 N HCl extractable Fe(II) remained in the column after the Cr(VI) reduction capacity of the column was exhausted, it is likely that a fraction of this easily available Fe(II) was not utilized for Cr(VI) reduction. It can also be seen from Figure 8 that the amount of total-Fe extractable with 0.25 N HCl + 0.25 N NH_2OH (Lovley and Phillips, 1987; Nyman et al., 2002), was approximately 10-fold higher than the bioavailable Fe(II) indicating that there was a significant amount of "bioavailable Fe(III)" in the columns, that was not microbially reduced. It is likely that some of this Fe(III) was produced by oxidation of Fe(II) during abiotic Fe(II)-mediated reduction of Cr(VI) (Wielinga et al., 2001).

Significantly higher amounts of Fe(II) were extracted by 2.5 N HCl than by 0.5 N HCl (Fig. 8), which indicates that an appreciable fraction of Fe(II) produced in the column, remained unavailable for Cr(VI) reduction. The total extractable Fe, measured using 2.25 N HCl + 0.25 N NH_2OH, was the highest among the four Fe measurements and shows that a large amount of Fe(III) remained within the columns.

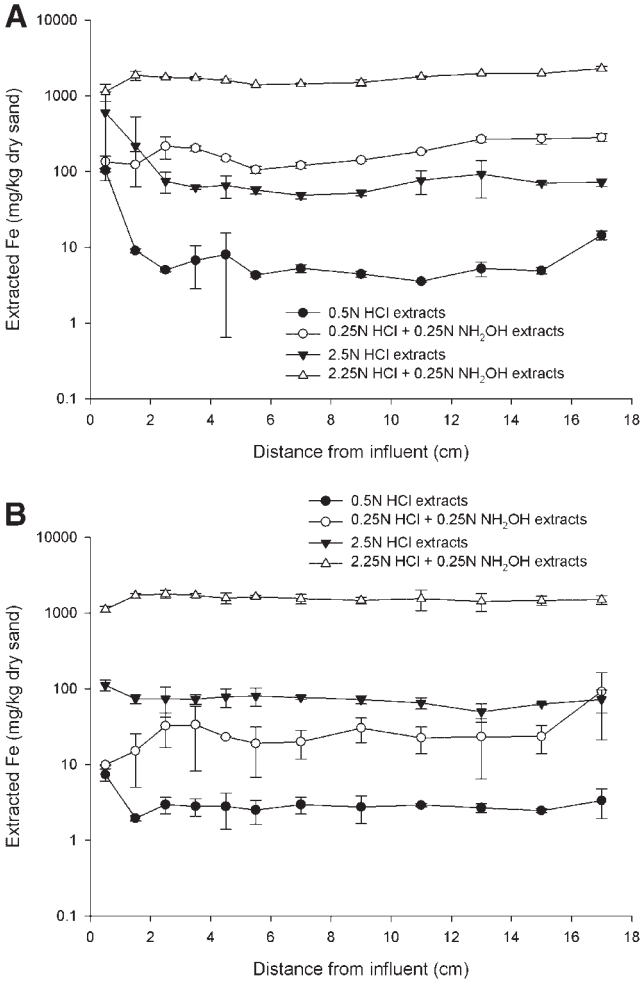

Figure 8. Solid phase extractable iron profiles for (**A**) column F1 and (**B**) column F2. Error bars indicate 95% confidence intervals of mean values from triplicate measurements.

Also, the Fe profiles in Figure 8 show that solid-phase Fe(II) concentrations were higher near the influent, while total-Fe values were lower. This suggests that Fe(III) reduction was higher near the influent, in agreement with observations of higher cell (protein) concentrations and Cr precipitation near the influent (Figs. 6 and 7).

Discussion

Tracer tests showed little or no retardation of Cr(VI) in either the quartz (Q) or iron coated sand (F) columns. Although iron oxides can adsorb anions and oxy anions, such as chromate (Schick and Lawrence, 1981), adsorption is significantly suppressed by the presence of common anionic constituents such as CO_3^{2-}, SO_4^{2-}, and SiO_4^{2-} (Zachara et al., 1987). During our experiments, it is likely that the ion exchange sites on the HFO surface were occupied by anions present in SGM during the 14 days growth phase and prevented CrO_4^{2-} adsorption during the subsequent Cr(VI) feed. Thus, in our experiments, delay in Cr(VI) breakthrough can be solely attributed to chemical and biochemical Cr(VI) reduction reactions.

ES6 cultures reduced Cr(VI) in the absence of nutrients in both the Q- and F-columns, although Cr(VI) reduction proceeded for much longer periods in the F-columns. Previous batch studies have shown that ES6 can reduce Fe(III) and Cr(VI) in the absence of external electron donors and it has been hypothesized that endogenous electron reserves, accumulated by ES6 during fermentative growth on substrates such as glucose, xylose, and sucrose, serve as the electron source for metal reduction (Sani et al., 2002; Viamajala et al., 2007). Cr(VI) reduction in the Q-columns, is consistent with this hypothesis and it is likely that internal electron donors were utilized to enzymatically reduce Cr(VI) in the absence of external carbon source. However, it is also possible that release of cellular materials due to cell lysis under starvation conditions (Van Loosdrecht and Henze, 1999) may have supplied the reductants for Cr(VI) reduction.

In the F-columns, the much higher Cr(VI) reduction observed indicates that mechanisms other than direct enzymatic reduction were also occurring. The significant Fe(III) reduction evidenced by effluent Fe(II) measurements, suggests that Fe(II)-mediated Cr(VI) reduction was likely the dominant mechanism in the F-columns. The correlation of Cr(VI) breakthrough with disappearance of effluent Fe(II), and the reported fast kinetics of Cr(VI) reduction by aqueous Fe(II) (Sedlak and Chan, 1997) indicate that reduction by dissolved Fe(II) was the dominant contributor. However, significant amounts of Cr(VI) reduction by surface-associated Fe(II) have previously been reported in batch (Anderson et al., 1994) and flow-through column studies (Nyman et al., 2002) and it is likely that a portion of Cr(VI) reduction observed in our tests was mediated by surface-associated Fe(II) as well.

While complete Cr(VI) reduction was observed when measurable Fe(II) was present in the effluent, a lower level of Cr(VI) reduction persisted for a significant period of time after the depletion of soluble Fe(II) in the F-column effluents (Fig. 4 and Table II). During this time, either small amounts of soluble Fe(II) were still being released from the column matrix and completely consumed by Cr(VI) or surface associated Fe(II) was involved in reaction with Cr(VI). If surface associated Fe(II) was reducing Cr(VI), it would appear that the reaction rates by this mechanism, after prolonged exposure to Cr(VI) and aqueous Fe(II), are low since only small amounts of Cr(VI) were consumed during this period (0.3–0.6 mg/L, Fig. 4). Cr(VI) reduction rates by surface-associated Fe(II) have been previously reported to decrease over time. Anderson et al. (1994), for instance, reported rapid initial kinetics followed by slower rates during tests with sediments containing Fe-minerals and attributed the decrease in reduction rate to diffusional limitations as Cr(VI) tries to access Fe(II) within the porous

structure of the mineral. In more recent studies, He and Traina (2005) also reported a similar decrease in Cr(VI) reduction rates over time with magnetite at neutral pH, where complete Cr(VI) removal required up to 400 h of incubation. Further, during Cr(VI) reduction tests with microbially reduced HFO, Nyman et al. (2002) noted that after rapid initial rates, slow Cr(VI) reduction persisted for long periods. The behavior seen during our tests is consistent with these previous observations.

In addition to slow rates of Cr(VI) reduction observed with Fe(II) containing solids, incomplete utilization of available Fe(II) has also been reported. Nyman et al. (2002) reported that during flow through tests in columns containing reduced HFO, only 1% of the available surface-associated Fe(II) was utilized for Cr(VI) reduction. Our results also indicate that a large amount of surface associated Fe(II) (extractable by 0.5 and 2.5 N HCl, Fig. 8) remained in the column after Cr(VI) reduction activity was depleted. Based on the mass of each column section and the extracted Fe concentrations therein, the cumulative Fe content of each column is shown in Table III. Since 0.5 N HCl extracts only the "loosely bound" Fe(II) while 2.5 N HCl extracts all the Fe(II) present in the system, it appears that a majority of Fe(II) that remained unreacted in the columns was "tightly associated" with the solid phase. Hansel et al. (2003a) showed that under advective flow conditions, ferrihydrite (structurally similar to HFO) reduction results in rapid conversion of the amorphous ferrihydrite to the crystalline magnetite (major) and goethite (minor) forms. Since magnetite incorporates a portion of Fe(II) into its crystal structure, this "fixed" fraction is not extractable by 0.5 N HCl and requires acid strengths of 2.5–3 N to extract (Jeon et al., 2003). Since our results show that the majority of solid-phase Fe(II) was extractable only with 2.5 N HCl, it is likely that sequestration of Fe(II) into crystalline mineral structure was at least partly responsible for its unavailability for Cr(VI) reduction.

In addition to the formation of magnetite, it is also likely that solid phase Fe(II) remained inaccessible due to passivation of the Fe(II)-containing surfaces. He and Traina (2005) showed that reduction of Cr(VI) by magnetite can cause formation of goethite and maghemite and speculated that deposition of these secondary phases on the mineral surface formed an insulating barrier which prevented electron transfer from Fe(II) contained in the deeper layers. Fe-Cr hydroxides ($Fe_{1-x}Cr_x(OH)_3$), formed during Fe(II) mediated Cr(VI) reduction (Hansel et al., 2003b; He and Traina, 2005), have also been postulated to form strong surface complexes on iron oxide and hydroxide surfaces (Kendelewicz et al., 1999) and might have also contributed to the inaccessibility of solid-phase Fe(II).

In addition to formation of secondary Fe(III) oxides and hydroxides, it is also possible that siderite ($FeCO_3$) was formed in our system due to the high concentration of carbonate buffer in our medium. While Hansel et al. (2003b) did not observe siderite formation during their experiments in carbonate buffer, Vázquez-Morillas et al. (2006) reported that siderite was formed during reduced ferrihydrite-mediated Cr(VI) reduction. Other reports have also established formation of siderite during microbial Fe reduction (e.g., Fredrickson et al., 1998 and references therein). Although these mineralogical analyses were not performed during our research, white precipitates were observed during solid phase sampling of the F-columns suggesting that some siderite might have formed on the HFO-coated sand surface. While siderite can reduce Cr(VI), previous work has suggested that only a small fraction of Fe(II) contained in siderite (approximately 7%) can be utilized for Cr(VI) reduction (Erdem et al., 2004). Further, siderite is soluble in 0.5 M HCl (Schnell et al., 1998) and it is therefore likely that at least part of the 0.5 M extractable Fe(II) detected in our systems (Fig. 8, Table III) was derived from unreacted siderite.

In addition to Fe(II) remaining in the columns at the end of the experiments, significant amounts of Fe(III) also remained unutilized. The majority of the Fe(III) remaining in the columns was extractable only with 2.5 N HCl + 0.25 N NH_2OH while only a small fraction of the total Fe(III) was extractable by 0.25 N HCl + 0.25 N NH_2OH (Fig. 8, Table III). Since amorphous Fe(III) is extractable by 0.5 N HCl (Schnell et al., 1998), it seems likely that most of the Fe(III) remaining in the system was associated with more crystalline minerals such as magnetite, goethite and maghemite that might have formed. $Fe_{1-x}Cr_x(OH)_3$ formed during Fe-mediated Cr(VI) reduction is amorphous (Wielinga et al., 2001) and therefore the Fe(III) extractable by 0.25 N HCl + 0.25 N NH_2OH was likely derived from these Cr-Fe hydroxides or unreduced HFO. To evaluate the relative abundance of Cr(III) and amorphous Fe(III), mole fractions of Cr(III) within the Cr(III)–$Fe(III)_{amorphous}$ mixture were evaluated and are shown in Figure 9. Most of the mole fraction values near the influent were >0.25, the minimum theoretical ratio likely to be present if Fe(II) reacted stoichiometrically with Cr(VI) to form

Table III. Summary of Fe masses extracted from column at the end of experiment.

		Fe(II) remaining in column (mg)		Total Fe remaining in column (mg)		Fe(III) remaining in column (mg) (total Fe–Fe(II))	
Column	Total effluent Fe (mg)	0.5 N HCl	2.5 N HCl	0.25 N HCl + 0.25 N NH_2OH	2.25 N HCl + 0.25 N NH_2OH	Amorphous	Crystalline
F1	30.90	1.35	12.40	21.58	197.12	20.23	184.72
F2	15.64	0.35	8.24	3.15	175.50	2.80	167.26

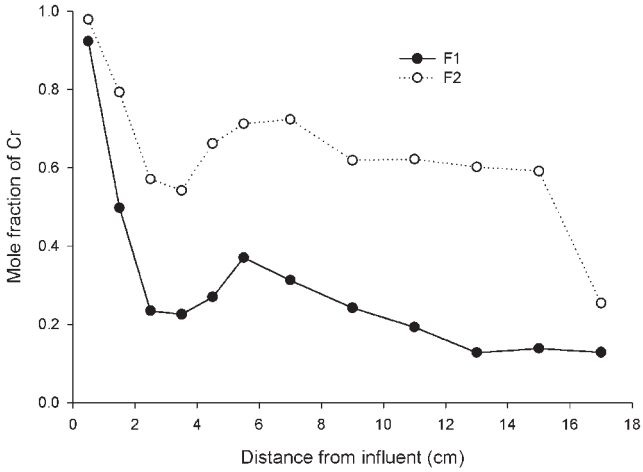

Figure 9. Mole fraction of Cr(III) in the Cr(III)–Fe(III) mixture extractable by 0.25 N HCl + 0.25 N NH_2OH.

$Fe_{0.75}Cr_{0.25}(OH)_3$. Hansel et al. (2003b) showed that as Fe(II)-mediated Cr(VI) reduction proceeds and Fe(III) within Cr-Fe hydroxides are repeatedly reduced enzymatically to produce more Fe(II) for Cr(VI) reduction, the hydroxide products become enriched in Cr relative to Fe and ultimately approach a pure $Cr(OH)_3 \cdot nH_2O$ phase. Figure 9 demonstrates that Cr existed as a nearly pure phase, relative to Fe(III), near the influent where a large number of cells were present and large amounts of Cr(VI) and Fe(III) depletion occurred suggesting that significant iron cycling occurred at the column entrance.

Fe(III) and Cr(VI) reduction during our column studies were likely enhanced by AQDS present in the medium (0.054 mM). Previous batch tests in our lab have shown that ES6 can reduce AQDS and that Cr(VI) and Fe(III) reduction rates by ES6 are higher in the presence of AQDS (unpublished data). Other researchers have also observed similar enhancement of metal reduction rates in the presence of AQDS (Fredrickson et al., 2000b; Lovley et al., 1996). However, the presence of AQDS alone cannot sustain Cr(VI) reduction for extended periods, as evident from the quartz sand column results (Fig. 2), and Fe(III) reduction provides the ability to significantly extend the effectiveness of the biobarrier. Humic substances are ubiquitous in terrestrial and aquatic environments and are likely to participate in electron transfer processes to Fe(III) in these environments (Lovley et al., 1996). The addition of humic substances as amendments to groundwater to facilitate Fe(III) and heavy metal reduction has also been suggested previously (Yates and Wandruszka, 1999).

After completion of the experiments, relative amounts of Cr(III) associated with the solid and liquid phases were evaluated and these results are shown in Table IV. Cr(VI) reduced (and theoretically equivalent to total Cr(III) produced) was calculated by subtracting the area under the effluent Cr(VI) plots (Figs. 2 and 4) from the amount of Cr(VI) fed. Cr(III) in the effluent was calculated by integrating (Cr_{tot}–Cr(VI)) values over time, again from Figures 2 and 4. As can be seen from Table IV, approximately 80% of the total Cr mass was accounted for and the approximately 20% unaccounted Cr mass was likely associated with effluent cells or abiotic colloids since effluent total Cr measurements were made on 0.22 μm filtered samples. However, it is interesting to note that a significant amount of apparently soluble Cr(III) leached out of the columns. The proportion of soluble Cr in the effluent was higher in the Q-columns when compared to the F-columns.

In the Q-columns, only ~45–50% of the reduced Cr was retained in the columns, while ~75–80% was retained in the F-columns. Although Cr(VI) reduction is commonly believed to form insoluble $Cr(OH)_3$ (Barnhart, 1997; Richard and Bourg, 1991), soluble organo-Cr(III) complexes can form when Cr(VI) is reduced in the presence of organic acids such as citrate, ascorbate, malate, pyruvate, etc. (Alam et al., 2006; Puzon et al., 2005). Since these organic acids are cellular metabolites, their release in our reactors might have led to formation of soluble Cr(III) complexes. Humic acids can also chelate cationic metals (Yates and Wandruszka, 1999) and it is possible that AQDS might have solubilized a portion of Cr(III). However, it is important to note that a smaller fraction of soluble Cr(III) was formed in the Fe-containing columns indicating that Fe(II)-mediated Cr(VI) reduction might lead to the preferential formation of insoluble Fe-$Cr(OH)_3$ precipitates and therefore afford better bioremediation results.

Implementation of biologically active PRBs offers several advantages over technologies that utilize Fe(0) or reductants such as dithionite. While zero-valent iron barriers are economical means of remediating shallow groundwater, the commonly practiced trench and fill methods are uneconomical at depths >12 m (Fortner, 1995). Groundwater in the deep subsurface could be remediated by injecting small Fe(0) particles either under high pressure or after fracturing

Table IV. Chromium mass balance data.

Column	Cr(VI) reduced (mg) (*A*)	Cr(III) remaining in column (mg) (*B*)	Soluble Cr(III) in effluent (mg) (*C*)	% Cr(III) retained in column ((*B*)/(*A*))	% Cr(III) recovered (((*B*) + (*C*))/(*A*))
Q1	1.47	0.64	0.51	43.5	78.2
Q2	1.43	0.71	0.45	49.6	81.1
F1	9.46	7.49	0.51	79.2	84.6
F2	5.90	6.12	0.37	76.8	83.1

the aquifer (Cantrell et al., 1997), but might also be uneconomical and limited by restricted transport of colloidal Fe(0). On the other hand, injection of chemical Fe(III) reductants (e.g., dithionite) might face hurdles in terms of regulatory approval and disposal of secondary wastes (Chilikapati et al., 2000; Istok et al., 1999). Another disadvantage of physico-chemical barriers is that they suffer from passivation and are difficult to reactivate after their reduction capacity has been exhausted (Vázquez-Morillas et al., 2006). Biologically active barriers, such as those containing stimulated *Cellulomonas*-like microorganisms can overcome both these hurdles. Since *Cellulomonas* spp. and other iron reducing organisms are naturally present in the subsurface (Viamajala et al., 2007), they can be stimulated in situ. Further, inexpensive carbon sources such as molasses or cheese whey can be used to stimulate these fermentative organisms instead of the more expensive organic acids required to more selectively grow DIRB. Additionally, even in the absence of continuous external electron sources or nutrients, these organisms can reduce Cr(VI) through direct enzymatic mechanisms or can facilitate the reduction process through generation of Fe(II) ensuring Cr(VI) reduction over long periods, as evidenced during this study. Thus, contaminant remediation does not have to rely on external carbon inputs or surface associated Fe(II), which might become inaccessible due to deposition of $Cr(OH)_3$ or formation of crystalline minerals. The continuous generation of Fe(II) at low rates should preserve the reducible Fe(III) content within the aquifer for longer periods, such that sufficient Fe(III) remains in the system for subsequent regeneration. In addition to establishment of new barriers, organisms like *Cellulomonas* could also be used to regenerate existing zero-valent iron barriers that have been passivated due to formation of amorphous and crystalline iron-minerals (Vázquez-Morillas et al., 2006).

Summary and Conclusions

This research demonstrates Cr(VI) and Fe(III) reduction by a *Cellulomonas* sp. strain ES6 in soil columns without a continuous supply of external electron donors. While Cr(VI) reduction occurred both in the presence and absence of Fe minerals, it persisted for much longer periods in the columns containing Fe(III) coated sand indicating that Fe(II)-mediated Cr(VI) reduction can be more effective than direct enzymatic Cr(VI) reduction alone. Our results show that fermentative organisms like *Cellulomonas* spp., once stimulated, can continue Fe(III) and Cr(VI) reduction and allow for the formation of sustainable reactive biobarriers. Further, it might be possible to maintain barrier activity by periodic addition of fresh substrate. Barrier performance can be assessed by monitoring Fe(II) levels downstream and decreased Fe(II) concentrations would provide a simple way of predicting imminent contaminant breakthrough. Thus, regeneration of the biofilm barrier could be initiated before Cr(VI) breakthrough. Formation and release of soluble Cr(III) is a concern when designing remediation systems for Cr(VI), and our results show that in systems containing Fe-minerals, the release of soluble Cr(III) species might remain below regulatory levels.

While our bench-scale column results are a proof of concept for this novel remediation strategy, further larger scale work in natural soils and sediments is required to fully assess this technology. Also, the cellular mechanisms by which *Cellulomonas* stores and utilizes internal electron reserves for metal reduction warrants further study.

This work was supported by the US Department of Energy, Office of Science, Natural and Accelerated Bioremediation Research (NABIR) Program under DOE-NE Idaho Operations Office contract number DE-AC07-05ID14517 and by grant DE-FG03-98ER62693. The work was also supported in part by the U.S. Department of Energy, Office of Science, Environmental Management Science Program (EMSP) under contracts DE-FG02-03ER63577, DE-FG02-03ER63582, DE-FG02-06ER64206, and by the Inland Northwest Research Alliance under contract WSU 005 and MSU 002.

References

Ackerley DF, Gonzalez CF, Park CH, Blake R, Keyhan A, Matin A. 2004. Chromate-reducing properties of soluble flavoproteins from *Pseudomonas putida* and *Escherichia coli*. Appl Environ Microbiol 70:873–888.

Alam M, Hossain MA, Yonge DR, Peyton BM, Petersen JN. 2006. Bioreduction of hexavalent chromium in flow-through quartz sand columns. J Environ Eng—ASCE 132:358–366.

Amonette JE, Workman DJ, Kennedy DW, Fruchter JS, Gorby YA. 2000. Dechlorination of carbon tetrachloride by Fe(II) associated with goethite. Environ Sci Technol 34:4606–4613.

Anderson LD, Kent D, Davis JA. 1994. Batch experiments characterizing the reduction of Cr(V1) using suboxic material from a mildly reducing sand and gravel aquifer. Environ Sci Technol 28:178–185.

Barnhart J. 1997. Chromium chemistry and implications for environmental fate and toxicity. J Soil Contam 6:561–568.

Benz M, Schink B, Brune A. 1998. Humic acid reduction by *Propionibacterium freudenreichii* and other fermenting bacteria. Appl Environ Microbiol 64:4507–4512.

Borch T, Inskeep WP, Harwood JA, Gerlach R. 2005. Impact of ferrihydrite and anthraquinone-2,6-disulphonate (AQDS) on the reductive transformation of 2,4,6-trinitrotoluene by a Gram positive fermenting bacterium. Environ Sci Technol 39:7126–7133.

Bradford MM. 1976. A rapid and sensitive method for the quantitation of microgram quantities of protein using the principle of protein-dye binding. Anal Biochem 72:248–254.

Burton FL, Tchobanoglous G, Stensel DH. 2003. Introduction to process analysis and selection. In: Wastewater Engineering: Treatment, Disposal, and Reuse. New York: McGraw-Hill, Inc., p 226–256.

Cantrell KJ, Kaplan DI, Gilmore TJ. 1997. Injection of colloidal Fe^0 particles in sand with shear-thinning fluids. J Environ Eng 123:786–791.

Cervantes FJ, de Bok FAM, Duong-Dac T, Stams AJM, Lettinga G, Field JA. 2002. Reduction of humic substances by halorespiring, sulphate-reducing and methanogenic microorganisms. Environ Microbiol 4:51–57.

Chardin B, Giudici-Orticoni MT, De Luca G, Guigliarelli B, Bruschi M. 2003. Hydrogenases in sulfate-reducing bacteria function as chromium reductase. Appl Microbiol Biotech 63:315–321.

Chilikapati A, Williams M, Yabusaki S, Cole C, Szecscody J. 2000. Optimal design of an in situ Fe(II) barrier: Transport limited reoxidation. Environ Sci Technol 34:5215–5221.

DeLeo PC, Ehrlich HL. 1994. Reduction of hexavalent chromium by *Pseudomonas fluorescens* LB300 in batch and continuous cultures. Appl Microbiol Biotechnol 40:756–759.

Dragun J. 1988. Element fixation in soil. In: The soil chemistry of hazardous materials. Greenbelt, MD: Hazardous Materials Control Research Institute, p 75-152.

Erbs M, Hansen HCB, Olsen CE. 1999. Reductive dechlorination of carbon tetrachloride using iron(II) iron(III) hydroxide sulfate (green rust). Environ Sci Technol 33:307–311.

Erdem M, Gur F, Tumen F. 2004. Cr(VI) reduction in aqueous solutions by siderite. J Haz Mat B 113:217–222.

Fortner B. 1995. Wall of iron purifies contaminated groundwater. Water Environ Technol 7:14–17.

Fredrickson JK, Zachara JM, Kennedy DW, Dong H, Onstott TC, Hinman NW, Li S. 1998. Biogenic iron mineralization accompanying the dissimilatory reduction of hydrous ferric oxide by a groundwater bacterium. Geochim Cosmochim Acta 62:3239–3257.

Fredrickson JK, Zachara JM, Kennedy DW, Duff MC, Gorby YA, Li SW, Krupka KM. 2000a. Reduction of U(VI) in goethite (alpha-FeOOH) suspensions by a dissimilatory metal-reducing bacterium. Geochim Cosmochim Acta 64:3085–3098.

Fredrickson JK, Kostandarithes HM, Li SW, Plymale AE, Daly MJ. 2000b. Reduction of Fe(III), Cr(VI), U(VI), and Tc(VII) by *Deinococcus radiodurans* R1. Appl Environ Microbiol 66:2006–2011.

Hansel CM, Benner SG, Neiss J, Dohnalkova A, Kukkadapu RK, Fendorf S. 2003a. Secondary mineralization pathways induced by dissimilatory iron reduction of ferrihydrite under advective flow. Geochim Cosmochim Acta 67:2977–2992.

Hansel CM, Wielinga BW, Fendorf S. 2003b. Structural and compositional evolution of Cr/Fe solids after indirect chromate reduction by dissimilatory iron-reducing bacteria. Geochim Cosmochim Acta 67:401–412.

He YT, Traina SJ. 2005. Cr(VI) reduction and immobilization by magnetite under alkaline pH conditions: The role of passivation. Environ Sci Technol 39:4499–4504.

Heijman CG, Grieder E, Holliger C, Schwarzenbach RP. 1995. Reduction of nitroaromatic compounds coupled to microbial iron reduction in laboratory aquifer columns. Environ Sci Technol 29:775–783.

Istok JD, Amonette JE, Cole CR, Fruchter JS, Humphrey MD, Szecscody JE, Teel SS, Vermeul VR, Williams MD, Yubasaki SB. 1999. In situ redox manipulation by dithionite injection: Intermediate-scale laboratory experiments. Ground Water 37:884–889.

Jeon BH, Dempsey BA, Burgos WD. 2003. Kinetics and mechanisms for reactions of Fe(II) with Iron(III) oxides. Environ Sci Technol 37:3309–3315.

Kendelewicz T, Liu P, Doyle CS, Brown GE, Jr., Nelson EJ, Chambers SA. 1999. X-ray absorption and photoemission study of the adsorption of aqueous Cr(VI) on single crystal hematite and magnetite surfaces. Surf Sci 424:219–231.

Langard S. 1980. Chromium. In: Waldron HA, editor. Metals in the environment. New York: Academy Press Inc, p 111–132.

Lee W, Batchelor B. 2002. Abiotic reductive dechlorination of chlorinated ethylenes by iron-bearing soil minerals—1. Pyrite and magnetite. Environ Sci Technol 36:5147–5154.

Lovley DR, Phillips EJP. 1987. Rapid assay for microbially reducible ferric iron aquatic sediments. Appl Environ Microbiol 53:1536–1540.

Lovley DR, Phillips EJP, Lonergan DJ. 1991. Enzymatic versus nonenzymatic mechanisms for Fe(III) reduction in aquatic sediments. Environ Sci Technol 25:1062–1067.

Lovley DR, Coates JD, Blunt-Harris EL, Phillips EJP, Woodward JC. 1996. Humic substances as electron acceptors for microbial respiration. Nature 382:445–448.

Nyman JL, Caccavo F, Cunningham AB, Gerlach R. 2002. Biogeochemical elimination of chromium (VI) from contaminated water. Bioremed J 6:39–55.

Patterson JW. 1985. Hexavalent chromium. In: Industrial wastewater treatment technology. Stoneham: Butterworth Publishers, p 53–76.

Puzon GJ, Roberts AG, Kramer DM, Xun L. 2005. Formation of soluble organo-chromium(III) complexes after chromate reduction in the presence of cellular organics. Environ Sci Technol 39:2811–2817.

Rege MA, Mills DA, Petersen JN, Sun Y, Yonge DR, Apel WA. 1998. Estimation of mass transport parameters in a column packed with BioSep beads. Biotech Tech 12:913–918.

Richard FC, Bourg ACM. 1991. Aqueous geochemistry of chromium: A review. Water Res 25:807–816.

Riley RG, Zachara JM, Wobber FJ. 1992. Chemical contaminants on DOE lands and selection of contaminant mixtures for subsurface science research. Washington DC: US Department of Energy, p ii–77.

Sani RK, Peyton BM, Smith WA, Apel WA, Petersen JN. 2002. Dissimilatory reduction of Cr(VI), Fe(III), and U(VI) by *Cellulomonas* isolates. Appl Microbiol Biotech 60:192–199.

Schick LL, Lawrence MM. 1981. Removal of hexavalent chromium from estuarine waters by model substrates and natural sediments. Environ Sci Technol 15:1482–1484.

Schmieman EA, Yonge DR, Rege MA, Petersen JN, Turick CE, Apel WA. 1998. Comparative kinetics of bacterial reduction of chromium. J Environ Eng 124:449–455.

Schnell S, Ratering S, Jansen KH. 1998. Simultaneous determination of iron(III), iron(II), and manganese(II) in environmental samples by ion chromatography. Environ Sci Technol 32:1530–1537.

Sedlak DL, Chan PG. 1997. Reduction of hexavalent chromium by ferrous iron. Geochim Cosmochim Acta 61:2185–2192.

Stearns DM, Belbruno JJ, Wetterhahn KE. 1995. A prediction of chromium (III) accumulation in humans from chromium dietary supplements. FASEB J 9:1650–1657.

Turick CE, Apel WA, Carmiol NS. 1996. Isolation of hexavalent chromium-reducing anaerobes from hexavalent-chromium-contaminated and noncontaminated environments. Appl Microbiol Biotechnol 44:683–688.

Van Loosdrecht MCM, Henze M. 1999. Maintenance, endogenous respiration, lysis, decay and predation. Water Sci Technol 39:107–117.

Vázquez-Morillas A, Vaca-Mier M, Alvarez PJ. 2006. Biological activation of hydrous ferric oxide for reduction of hexavalent chromium in the presence of different anions. Eur J Soil Biol 42:99–106.

Viamajala S, Peyton BM, Apel WA, Petersen JN. 2002. Chromate/nitrite interactions in *Shewanella oneidensis* MR-1: Evidence for multiple hexavalent chromium [Cr(VI)] reduction mechanisms dependent on physiological growth conditions. Biotech Bioeng 78:770–778.

Viamajala S, Smith WA, Sani RK, Apel WA, Petersen JN, Neal AL, Roberto FF, Newby DT, Peyton BM. 2007. Isolation and characterization of Cr(VI) reducing *Cellulomonas* spp from subsurface soils: Implications for long term chromate reduction. Biores Technol 98: 612–622.

Wielinga B, Mizuba MM, Hansel CM, Fendorf S. 2001. Iron promoted reduction of chromate by dissimilatory iron-reducing bacteria. Environ Sci Technol 35:522–527.

World Health Organization. 1990. IARC Monographs on the evaluation of carcinogenic risks to humans: Chromium, nickel and welding. France: Lyons, p 49–256.

Yates LM III, Wandruszka RV. 1999. Decontamination of polluted water by treatment with a crude humic acid blend. Environ Sci Technol 33:2076–2080.

Zachara ZA, Girvin DC, Schmidt RL, Resch TC. 1987. Chromate adsorption on amorphous iron oxyhydroxide in the presence of major groundwater ions. Environ Sci Technol 21:589–594.